MEG Covariance Difference Analysis: A Method to Extract Target Source Activities by Using Task and Control Measurements

Kensuke Sekihara,* *Member, IEEE*, David Poeppel, Alec Marantz, Colin Phillips, Hideaki Koizumi, and Yasushi Miyashita

***Abstract*— A method is proposed for extracting target dipole-source activities from two sets of evoked magnetoencephalographic (MEG) data, one measured using task stimuli and the other using control stimuli. The difference matrix between the two covariance matrices obtained from these two measurements is calculated, and a procedure similar to the MEG-multiple signal classification (MUSIC) algorithm is applied to this difference matrix to extract the target dipole-source configuration. This configuration corresponds to the source-configuration difference between the two measurements. Computer simulation verified the validity of the proposed method. The method was applied to actual evoked-field data obtained from simulated task-and-control experiments. In these measurements, a combination of auditory and somatosensory stimuli was used as the task stimulus and the somatosensory stimulus alone was used as the control stimulus. The proposed covariance difference analysis successfully extracted the target auditory source and eliminated the disturbance from the somatosensory sources.**

***Index Terms*— Array signal processing, biomagnetics, biomedical electromagnetic imaging, biomedical signal processing, functional brain imaging, inverse problems.**

I. Introduction

NONINVASIVE measurement of human brain functions is attracting much interest. Such measurements often use various kinds of sensory stimuli, especially when measuring higher-order cognitive functions. One general difficulty here is extracting information on the target brain activity, which is of primary interest in the experiments. This is partly because spontaneous brain activity overlaps the target activity. More substantially, sensory stimuli generally elicit not only the target cortical activities but also other activities that are not the main interest in the experiment. The existence of these other activities can make interpreting the experimental results difficult.

Therefore, in most studies using positron emission tomography (PET) or functional magnetic resonance imaging (fMRI), neuropsychologists carefully design their experiments to extract only the target activities. A common example for such experimental designs contains two kinds of stimuli: a task stimulus and a control stimulus. The task stimulus generally elicits the target cortical activities as well as other activities associated with them. The control stimulus is designed to elicit only these associated activities. Then, by calculating the difference between the images measured with each kind of stimulus, the target activities can be extracted.

Among the various modalities that provide functional brain images, magnetoencephalography (MEG) [1] has a distinct advantage—it can provide a temporal resolution of less than 1 ms. MEG measurements have been used to localize various kinds of cortical activities including the primary sensory areas [2]–[4], spontaneous activities [5], and higher-order cortical activities [6], [7]. However, experiments using task and control stimuli are relatively rare in MEG, probably because appropriate data-analysis methods for such measurements do not exist.

In this paper we propose a novel method for extracting the target source information from evoked MEG data measured with task and control stimuli. This method is based on the covariance difference algorithm originally proposed to eliminate the influence of nonwhite noise with unknown statistical properties in sonar-signal processing [8]. Two sets of data are measured under different stimulus conditions; the difference between the covariance matrices obtained from these two measurements is then calculated. A procedure similar to the MEG-multiple signal classification (MUSIC) algorithm [9] is applied to this difference matrix to extract the target source configuration, which corresponds to the source-configuration difference between the two measurements.

After describing the proposed method, we present results from computer simulation and from application to evoked-response measurements simulating task-and-control-type experiments. Both sets of results strongly suggest that the proposed algorithm is effective. In this paper, we use plain italics to indicate scalars, lower-case boldface italics to indicate vectors, and upper-case boldface italics to indicate matrices. The

Manuscript received January 16, 1997; revised July 2, 1997. *Asterisk indicates corresponding author.*

*K. Sekihara, is with the Mind Articulation Project, Japan Science and Technology Corporation (JST), Yushima 4-9-2, Bunkyo, Tokyo 113 Japan (e-mail: ksekiha@po.iijnet.or.jp).

D. Poeppel is with the Biomagnetic Imaging Laboratory, University of California, San Francisco, CA 94143-0628 USA.

A. Marantz is with the Department of Linguistics, Massachusetts Institute of Technology, Cambridge, MA 02139 USA.

C. Phillips is with Linguistic and Cognitive Science, University of Delaware, Newark, DE 19716 USA.

H. Koizumi is with the Mind Articulation Project, Japan Science and Technology Corporation (JST), Tokyo 113 Japan.

Y. Miyashita is with the Department of Physiology, The University of Tokyo, School of Medicine, Hongo, Tokyo 113 Japan. He is also with the Mind Articulation Project, Japan Science and Technology Corporation (JST), Tokyo 113 Japan.

Publisher Item Identifier S 0018-9294(98)00248-1.

superscript T indicates the matrix transpose. The eigenvalues are numbered in decreasing order. For simplicity, we omit the explicit time notation unless any confusion due to this omission arises.

II. Method

A. Definitions

We define the magnetic field measured by the mth detector coil at time t_k as $b_m(t_k)$, and vector $\boldsymbol{b}(t_k) = (b_1(t_k), b_2(t_k), \cdots, b_M(t_k))^T$ as a set of measured data at t_k where $k = 1, 2, \cdots, K$. Here, K is the total number of time points, and M is the total number of detector coils. The spatio-temporal data matrix $\boldsymbol{B}$ is defined as $\boldsymbol{B} = [\boldsymbol{b}(t_1, \boldsymbol{b}(t_2), \cdots, \boldsymbol{b}(t_K)]$. We assume that a total of P current-dipole sources generate a biomagnetic field. The spherical homogeneous conductor model [10] is assumed, and two tangential components, the ϕ and θ components, of the source moment are considered. The magnitude of the pth dipole-source moment is defined as $S_p(t_k)$. Its orientation is defined as the dipole's normal vector $\boldsymbol{\eta}_p(t_k) = (\eta_p^{\phi}(t_k), \eta_p^{\theta}(t_k))$, where $||\boldsymbol{\eta}(t_k)|| = 1$. The source magnitude vector at t_k is defined as $\boldsymbol{s}(t_k) = (S_1(t_k), S_2(t_k), \cdots, S_P(t_k))^T$. The source temporal behavior $\boldsymbol{S}$ is defined as $\boldsymbol{S} = [\boldsymbol{s}(t_1), \boldsymbol{s}(t_2), \cdots, \boldsymbol{s}(t_K)]$.

The lead field vectors for the ϕ and θ components of the pth source are defined as $\boldsymbol{l}_p^{\phi} = (l_{p,1}^{\phi}, l_{p,2}^{\phi}, \cdots, l_{p,M}^{\phi})^T$ and $\boldsymbol{l}_p^{\theta} = (l_{p,1}^{\theta}, l_{p,2}^{\theta}, \cdots, l_{p,M}^{\theta})^T$. We define the lead field vector for the pth source at t_k as $\boldsymbol{l}_p(t_k)$. This $\boldsymbol{l}_p(t_k)$ is obtained using

$$\boldsymbol{l}_p(t_k) = \eta_p^{\phi}(t_k)\boldsymbol{l}_p^{\phi} + \eta_p^{\theta}(t_k)\boldsymbol{l}_p^{\theta}. \tag{1}$$

The lead field matrix for the entire set of P dipole sources is defined as

$$L(t_k) = [\boldsymbol{l}_1(t_k), \boldsymbol{l}_2(t_k), \cdots, \boldsymbol{l}_P(t_k)]. \tag{2}$$

For simplicity, we assume in this paper that all dipole sources have fixed orientations during measurement. Because $\boldsymbol{L}(t_k)$ becomes time-independent under this assumption, the relationship between $\boldsymbol{B}$ and $\boldsymbol{S}$ can be expressed, using the simpler notation $\boldsymbol{L}$

$$\boldsymbol{B} = \boldsymbol{L}\boldsymbol{S} + \boldsymbol{N}. \tag{3}$$

$\boldsymbol{N}$ is the noise matrix defined by $\boldsymbol{N} = [\boldsymbol{n}(t_1), \boldsymbol{n}(t_2), \cdots, \boldsymbol{n}(t_K)]$, where $\boldsymbol{n}(t_k)$ is the additive noise at time t_k. The conventional way of estimating the locations of the dipole sources is based on minimizing the least squares cost function

$$\mathcal{F} = ||\boldsymbol{B} - \hat{\boldsymbol{L}}\hat{\boldsymbol{S}}||^2 = ||\big(I - \hat{\boldsymbol{L}}\big(\hat{\boldsymbol{L}}^T\hat{\boldsymbol{L}}\big)^{-1}\hat{\boldsymbol{L}}^T\big)\boldsymbol{B})||^2. \tag{4}$$

Here, I is the unit matrix, and the estimates of L and S are denoted as $\hat{L}$ and $\hat{S}$, respectively. This minimization requires a $3P$-dimensional search, where P is again the number of sources. Generally, for such a highly multidimensional optimization search, there is no guarantee of obtaining a correct solution unless we can set the initial estimate very close to the true solution.

B. MUSIC Algorithm

The MUSIC algorithm approach has recently been introduced [9], [11], [12] to avoid this highly multidimensional search. A distinct advantage of this algorithm is that regardless of the number of dipole sources, it gives a suboptimal estimate of the source locations by using only a three-dimensional search in the solution space. We define the measured-data covariance matrix as $\boldsymbol{R}$, the covariance matrix of the dipole-source activities as $\boldsymbol{Q}$. Using (3), we get

$$\boldsymbol{R} \approx \boldsymbol{B}\boldsymbol{B}^T = \boldsymbol{L}(\boldsymbol{S}\boldsymbol{S}^T)\boldsymbol{L}^T + \boldsymbol{N}\boldsymbol{N}^T \approx \boldsymbol{L}(\boldsymbol{Q})\boldsymbol{L}^T + \sigma^2\boldsymbol{I} \tag{5}$$

where it is assumed that the noise in the measured data is white Gaussian noise with variance σ^2, and that the noise is uncorrelated with the signal. Unless some of the source activities are perfectly correlated with each other, the rank of $\boldsymbol{R}$ is equal to the number of sources P. Therefore, $\boldsymbol{R}$ has P eigenvalues greater than σ^2 and $M - P$ eigenvalues equal to σ^2. We denote the eigenvectors of $\boldsymbol{R}$ as $\{\boldsymbol{e}_j\}$, where $j = 1, 2, \cdots, M$, and define matrices $\boldsymbol{E}_S$ and $\boldsymbol{E}_N$ as $\boldsymbol{E}_S = [\boldsymbol{e}_1, \cdots, \boldsymbol{e}_P]$ and $\boldsymbol{E}_N = [\boldsymbol{e}_{P+1}, \cdots, \boldsymbol{e}_M]$. The span of the columns in $\boldsymbol{E}_S$ is called the signal subspace and that in $\boldsymbol{E}_N$ called the noise subspace.

To estimate the locations of the dipole sources $(\boldsymbol{x}_1, \boldsymbol{x}_2, \cdots, \boldsymbol{x}_P)$, the MUSIC algorithm takes advantage of the fact that the lead field vector at each $\boldsymbol{x}_p$ is orthogonal to the noise subspace. Namely

$$\boldsymbol{L}^T\boldsymbol{e}_j = 0 \quad \text{for} \quad j = P+1, \cdots, M. \tag{6}$$

Thus, the source locations can be obtained by checking the orthogonality between the lead field vector and the noise subspace projector, $\boldsymbol{E}_N\boldsymbol{E}_N^T$. The measure that evaluates this orthogonality is called the MUSIC localizer, and is proposed to be [9]

$$J(\boldsymbol{x}) = 1/\lambda_{\min}(\overline{\boldsymbol{L}}(\boldsymbol{x})^T\boldsymbol{E}_N\boldsymbol{E}_N^T\overline{\boldsymbol{L}}(\boldsymbol{x}), \overline{\boldsymbol{L}}(\boldsymbol{x})^T\overline{\boldsymbol{L}}(\boldsymbol{x})) \tag{7}$$

where $\lambda_{\min}(\cdot, \cdot)$ indicates the generalized minimum eigenvalue of the matrix pair given in parenthesis. In this equation, $\overline{\boldsymbol{L}}(\boldsymbol{x})$ is expressed as $\overline{\boldsymbol{L}}(\boldsymbol{x}) = [\boldsymbol{l}_{\phi}(\boldsymbol{x}), \boldsymbol{l}_{\theta}(\boldsymbol{x})]$ where $\boldsymbol{l}_{\phi}(\boldsymbol{x})$ and $\boldsymbol{l}_{\theta}(\boldsymbol{x})$ are the lead field vectors for the ϕ and θ components of a source at $\boldsymbol{x}$.

The MUSIC localizer is calculated in a volume where sources can exist, and each location where the localizer reaches a peak is chosen as the location of one dipole source. Note that the localizer shown in (7) is derived under the assumption that the source orientations are fixed during measurement. It has been proven, however, that this localizer is also effective for dipole sources whose orientations vary during measurement [9]. It is also worth noting that the eigenvector corresponding to the minimum eigenvalue in (7) gives the estimate of the dipole-source orientation.

C. Covariance Difference Analysis

The essence of covariance difference analysis is calculating the difference between covariance matrices obtained from two measurements with different stimulus conditions. This analysis provides the difference in source distributions between the two

measurements, and thus is an appropriate tool for analyzing the data taken in MEG measurements with a pair of task-and-control stimulus conditions.

We assume that P_T sources are elicited by the task stimulus and that, among these P_T sources, P_C sources are also elicited by the control stimulus. In this paper, the sources elicited only by the task stimulus and not by the control stimulus are called the target sources and the sources elicited by the control stimulus are called the control sources. We define the number of target sources as P_S, such that $P_S = P_T - P_C$. The covariance matrix for the task measurement, $\boldsymbol{R}_T$, can be expressed as

$$\boldsymbol{R}_T = [\boldsymbol{l}_1, \boldsymbol{l}_2, \cdots, \boldsymbol{l}_{P_T}]\boldsymbol{Q}_T[\boldsymbol{l}_1, \boldsymbol{l}_2, \cdots, \boldsymbol{l}_{P_T}]^T + \boldsymbol{W}_T \quad (8)$$

where $\boldsymbol{Q}_T$ and $\boldsymbol{W}_T$, respectively, are the source and noise covariance matrices for the task condition. The covariance matrix for the control measurement, $\boldsymbol{R}_C$, is expressed as

$$\boldsymbol{R}_C = [\boldsymbol{l}_1, \boldsymbol{l}_2, \cdots, \boldsymbol{l}_{P_C}]\boldsymbol{Q}_C[\boldsymbol{l}_1, \boldsymbol{l}_2, \cdots, \boldsymbol{l}_{P_C}]^T + \boldsymbol{W}_C \quad (9)$$

where $\boldsymbol{Q}_C$ and $\boldsymbol{W}_C$ are the source and noise covariance matrices for the control condition.

To make the covariance difference algorithm valid, we need two assumptions: first, the correlation between the target sources and the control sources are negligibly small, and second, the noise statistical property remains unchanged between the two measurements. Under the first assumption, we have

$$\boldsymbol{Q}_T = \begin{bmatrix} \boldsymbol{Q}_S & \boldsymbol{O}_{P_S}^{P_C} \\ \boldsymbol{O}_{P_C}^{P_S} & \boldsymbol{Q}_C \end{bmatrix}. \quad (10)$$

Here, $\boldsymbol{O}_\mu^\nu$ is a $\mu \times \nu$ matrix with all of its elements equal to zero. The covariance matrix for the target sources, $\boldsymbol{Q}_S$, is a $P_S \times P_S$ matrix explicitly given by

$$\boldsymbol{Q}_S = \begin{bmatrix} \langle S_1^2 \rangle & \cdots & \langle S_1 S_{P_S} \rangle \\ \vdots & \ddots & \vdots \\ \langle S_{P_S} S_1 \rangle & \cdots & \langle S_{P_S}^2 \rangle \end{bmatrix}. \quad (11)$$

The covariance matrix for the control sources, $\boldsymbol{Q}_C$, is a $P_C \times P_C$ matrix given by

$$\boldsymbol{Q}_C = \begin{bmatrix} \langle S_{P_S+1}^2 \rangle & \cdots & \langle S_{P_S+1} S_{P_T} \rangle \\ \vdots & \ddots & \vdots \\ \langle S_{P_T} S_{P_S+1} \rangle & \cdots & \langle S_{P_T}^2 \rangle \end{bmatrix}. \quad (12)$$

The second assumption leads to $\boldsymbol{W}_T = \boldsymbol{W}_C$. Therefore $\boldsymbol{\Delta R}$, which is the difference between $\boldsymbol{R}_T$ and $\boldsymbol{R}_C$, can be expressed as

$$\boldsymbol{\Delta R} = \boldsymbol{R}_T - \boldsymbol{R}_C = [\boldsymbol{l}_1, \boldsymbol{l}_2, \cdots, \boldsymbol{l}_{P_S}]\boldsymbol{Q}_S[\boldsymbol{l}_1, \boldsymbol{l}_2, \cdots, \boldsymbol{l}_{P_S}]^T. \quad (13)$$

It was shown in [8] that $\boldsymbol{\Delta R}$ has P_S nonzero eigenvalues and $M - P_S$ zero-level eigenvalues, and that eigenvectors corresponding to zero-level eigenvalues are orthogonal to the lead field vector at the target source locations. That is, defining such eigenvectors as $\boldsymbol{e}'_j$, the relationship

$$[\boldsymbol{l}_1, \boldsymbol{l}_2, \cdots, \boldsymbol{l}_{P_S}]^T \boldsymbol{e}'_j = 0 \quad \text{for} \quad j = P_S + 1, \cdots, M \quad (14)$$

holds true. This relationship corresponds to the orthogonality relationship shown in (6) for the standard MUSIC algorithm. Thus, corresponding to the localizer in the standard MUSIC algorithm shown in (7), the locations of the target sources can be obtained by scanning the localizer calculated from

$$J(\boldsymbol{x}) = 1/\lambda_{\min}(\overline{\boldsymbol{L}}(\boldsymbol{x})^T \boldsymbol{E}_Z \boldsymbol{E}_Z^T \overline{\boldsymbol{L}}(\boldsymbol{x}), \overline{\boldsymbol{L}}(\boldsymbol{x})^T \overline{\boldsymbol{L}}(\boldsymbol{x})) \quad (15)$$

where $\boldsymbol{E}_Z = [\boldsymbol{e}'_{P_S+1}, \cdots, \boldsymbol{e}'_M]$.

In the above discussion, we made the assumption that all the control sources are activated by the task stimulus. This may not always be true. That is, some control sources may not appear in the task stimulus condition. The covariance difference analysis, however, is still effective in such cases if the condition described below is satisfied.

Let us assume that, among the P_C control sources, P_D sources are only activated in the control stimulus condition and $\tilde{P}_D$ sources are activated both in the task and the control conditions. A number from P_S+1 to P_S+P_D is given to each source in the first group of control sources. That is, S_j where $j = P_S + 1, \cdots, P_S + P_D$ represent the moment magnitudes of the sources in this group. A number from $P_S + P_D + 1$ to $P_S + P_C$ is given to each source in the second group, and their moment magnitudes are represented by S_j, where $j = P_S + P_D + 1, \cdots, P_S + P_C$. Note that the relationship $P_C = P_D + \tilde{P}_D$ holds.

The covariance matrix for the control sources activated only by the control stimulus, $\boldsymbol{Q}_D$, is thus given by

$$\boldsymbol{Q}_D = \begin{bmatrix} \langle S_{P_S+1}^2 \rangle & \cdots & \langle S_{P_S+1} S_{P_S+P_D} \rangle \\ \vdots & \ddots & \vdots \\ \langle S_{P_S+P_D} S_{P_S+1} \rangle & \cdots & \langle S_{P_S+P_D}^2 \rangle \end{bmatrix}. \quad (16)$$

The covariance matrix for the control sources activated by both the task and control stimulus, $\tilde{\boldsymbol{Q}}_D$, is given by

$$\tilde{\boldsymbol{Q}}_D = \begin{bmatrix} \langle S_{P_S+P_D+1}^2 \rangle & \cdots & \langle S_{P_S+P_D+1} S_{P_S+P_C} \rangle \\ \vdots & \ddots & \vdots \\ \langle S_{P_S+P_C} S_{P_S+P_D+1} \rangle & \cdots & \langle S_{P_S+P_C}^2 \rangle \end{bmatrix}. \quad (17)$$

Using $\tilde{\boldsymbol{Q}}_D$, the source-covariance matrix for the task stimulus condition can be expressed as

$$\boldsymbol{Q}_T = \begin{bmatrix} \boldsymbol{Q}_S & \boldsymbol{O}_{P_S}^{\tilde{P}_D} \\ \boldsymbol{O}_{\tilde{P}_D}^{P_S} & \tilde{\boldsymbol{Q}}_D \end{bmatrix}. \quad (18)$$

At this point, we make further assumption that the correlation between the two group of the control sources is negligibly small. Then, the source-covariance matrix for the control stimulus condition is given by

$$\boldsymbol{Q}_C = \begin{bmatrix} \boldsymbol{Q}_D & \boldsymbol{O}_{P_D}^{\tilde{P}_D} \\ \boldsymbol{O}_{\tilde{P}_D}^{P_D} & \tilde{\boldsymbol{Q}}_D \end{bmatrix}. \quad (19)$$

Thus, in this case, the difference matrix $\boldsymbol{\Delta R}$ can be expressed as

$$\boldsymbol{\Delta R} = \boldsymbol{R}_T - \boldsymbol{R}_C = [\boldsymbol{l}_1, \cdots, \boldsymbol{l}_{P_S}, \boldsymbol{l}_{P_S+1}, \cdots, \boldsymbol{l}_{P_S+P_D}] \cdot \boldsymbol{\Delta Q}[\boldsymbol{l}_1, \cdots, \boldsymbol{l}_{P_S}, \boldsymbol{l}_{P_S+1}, \cdots, \boldsymbol{l}_{P_S+P_D}]^T \quad (20)$$

where

$$\Delta Q = \begin{bmatrix} Q_S & O_{P_S}^{P_D} \\ O_{P_D}^{P_S} & -Q_D \end{bmatrix}. \tag{21}$$

It can be shown that the zero-level eigenvectors of ΔR are orthogonal to $[l_1, \cdots, l_{P_S+P_D}]$ [8]. That is, a localizer search using (15) not only detects the target sources but also the control sources that are activated only by the control stimulus. These two groups of sources can, however, be discriminated by checking the signs of the diagonal elements in matrix ΔQ, which can be estimated using

$$\widehat{\Delta Q} = \left[(L^T L)^{-1} L^T\right] \Delta R \left[(L^T L)^{-1} L^T\right]^T \tag{22}$$

where

$$L = [l_1, \cdots, l_{P_S+P_D}].$$

To calculate L, the orientations of the dipole sources need to be estimated using the eigenvector corresponding to the smallest eigenvalue in (15). An example of applying (22) to discriminate the two groups of sources will be presented in Section III-D.

D. Summary of Algorithm

The covariance difference algorithm is summarized as follows.

Step 1) The covariance matrices of the measured spatio-temporal data are calculated for the task and control measurements. Then, the difference matrix between these two covariance matrices is calculated.

Step 2) Eigen-decomposition of this difference matrix is performed, and the subspace spanned by zero-level eigenvectors is defined by separating the zero-level eigenvalues from the nonzero eigenvalues.

Step 3) The localizer defined by (15) is calculated throughout the field of view, and each location where $J(x)$ reaches a peak is determined to be the location of one dipole source.

Step 4) When it is possible that the results obtained in Step 3 contain control source locations, the signs of the diagonal elements of ΔQ are checked using (22) to separate the target sources from control sources.

III. Computer Simulation

A. General Data-Generation Conditions

We used computer simulation to test the validity of the proposed method. A 37-channel magnetometer whose coil alignment was the same as that of the Magnes biomagnetic measurement system (Biomagnetic Technologies Inc., San Diego) was assumed. The z direction was defined as the direction perpendicular to the plane of the detector coil located at the center of the coil alignment, and z was equal to zero at this coil plane. The values of the spatial coordinates (x, y, z) are expressed in centimeters. Three signal dipole sources were assumed to exist on a plane defined as $y = 1.0$: the first dipole source was at $(-1.1, 1.0, -5.6)$, the second was at $(2.8, 1.0, -5.4)$, and the third was at $(4.5, 1.0, -7.3)$. The source and detector configuration for this simulation is shown schematically in Fig. 1.

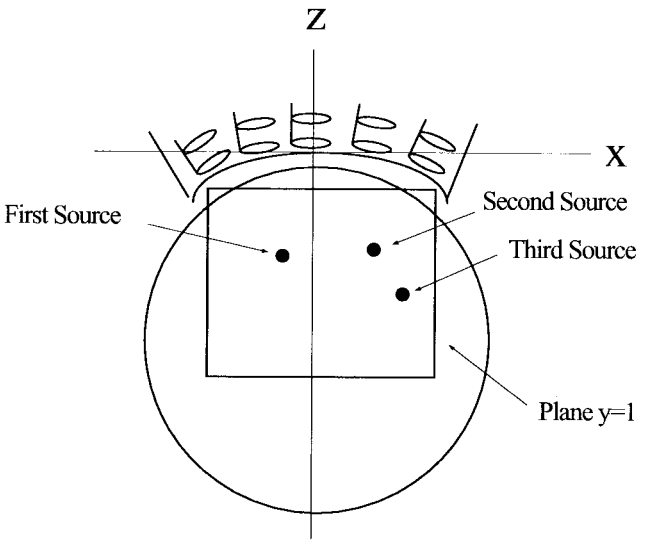

Fig. 1. Source and detector configuration assumed in computer simulation.

The spherical homogeneous conductor model [10] with the origin set at $(1.0, 1.0, -10)$ was used in this computer simulation. The simulated magnetic field was calculated at 1-ms intervals from 0 to 400 ms. To generate the simulated biomagnetic field, the ϕ components of these sources were modeled using exponentially damped sinusoidal functions, and the θ components were set to zero. The waveforms assigned to each ϕ component of the three sources are shown in Fig. 2. Here, the correlation coefficients between any pair of the three waveforms were less than 0.3.

Uncorrelated Gaussian noise was added to make the final signal-to-noise ratio (SNR) equal to 0.3 for the single-epoch data in the task condition. The SNR was defined by the ratio of the Frobenius norm of the signal-magnetic-field data matrix to that of the noise matrix. One hundred sets of the magnetic-field data were generated and averaged to create the magnetic field data used for the source estimation. The final SNR of this averaged field data was approximately three for the task condition.

B. Comparison with the Waveform-Subtraction Method

We first assumed that the task condition activates all three sources and that the control condition activates only the first and third sources. In this case, the second source is the target source. In actual task-and-control-type measurements, the onset of the control-source response may differ between the task and control measurements. To take this possibility into account, the onset of control-source activation was set to be delayed by 30 ms in the control measurement. The activation waveforms shown by the solid lines in Fig. 2 are used in the task condition and those shown by the broken lines are used in the control condition. The averaged magnetic-fields for the

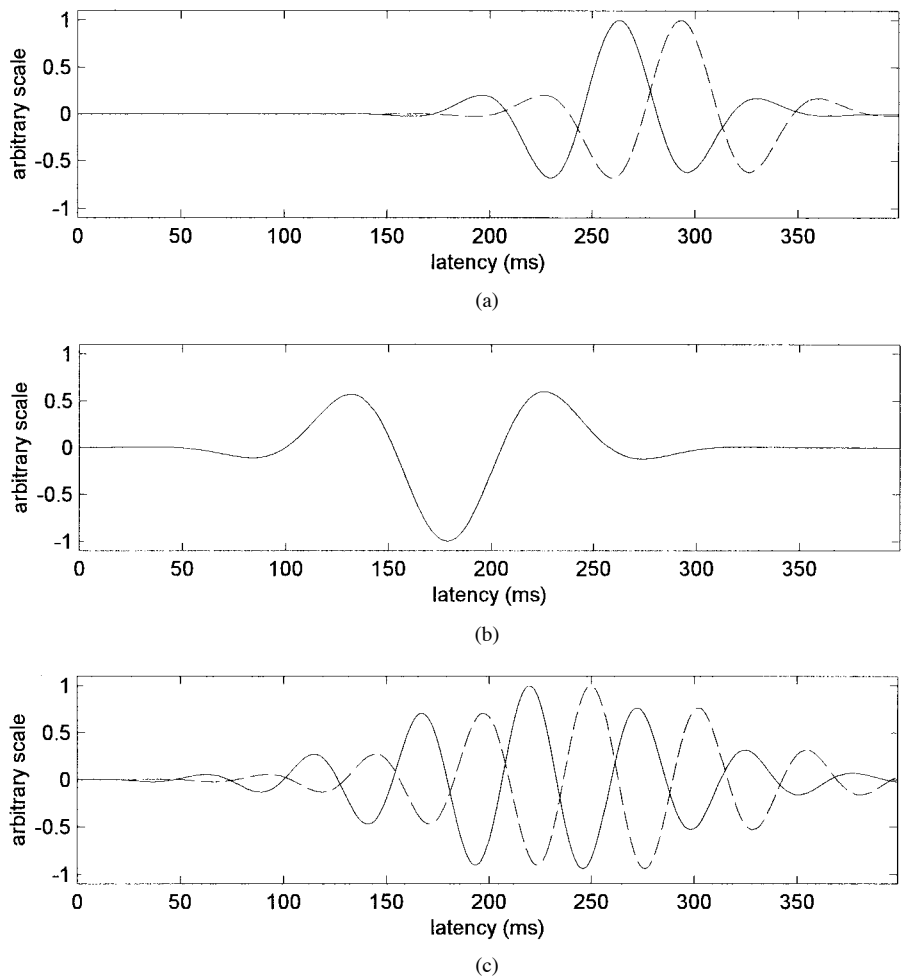

Fig. 2. The waveforms assigned to the ϕ components of (a) the first, (b) the second, and (c) the third source in the computer simulation. In Section III-B, the waveforms indicated by the solid lines are used in the task condition and those by the broken lines in the control condition.

task and control conditions are shown in Fig. 3(a) and (b). One of the single-epoch data is shown in Fig. 3(c).

The standard MUSIC localizer in (7) was applied to the averaged field data; the results of calculating the localizer on the $y = 1.0$ plane are shown in Fig. 4(a) and (b). Fig. 4(a) shows the results for the task condition and (b) shows those for the control condition. The contours in these figures show the relative value of the localizer, and each area where the localizer reaches a peak is considered to be the location of one dipole source. In Fig. 4(a) the localizer clearly detects the three signal sources, and in Fig. 4(b) it clearly detects the first and third sources. The results of applying covariance difference analysis are shown in Fig. 4(c). In this case, only the target source (the second source) remains—the influence of the control sources (the first and third sources) has been completely eliminated.

A naive way to extract information about the target activity from the task and control measurements is to directly subtract the field waveform elicited under the control condition from that under the task condition. The results of this simple waveform subtraction are shown in Fig. 4(d). Here, the control field waveform was subtracted from the task waveform, and the standard MUSIC localizer [(7)] was applied to this subtracted waveform. These results show that the simple subtraction method cannot separate the target source activity from the control activities due to the 30-ms time offset existing in the control source activations between the two conditions. A comparison between Fig. 4(c) and (d) clearly demonstrates the effectiveness of the proposed covariance difference analysis.

C. Effects of Strong Correlation Between Task and Control Sources

We conducted the computer simulation when the target source had a strong correlation with one of the control sources. The waveform indicated in Fig. 2(a) was assigned to both the first and second sources. The same data generation procedure as in Section III-B was repeated, and the covariance difference analysis was applied to the generated field data. The results are shown in Fig. 5. Here, the elimination of the control source influence obviously failed. These results demonstrate that the proposed covariance difference algorithm is not effective when strong correlation exists between the task and control sources.

D. Influence of a Control Source not Elicited in the Task Condition

We next assumed that the task condition activates the first and third sources and that the control condition activates the

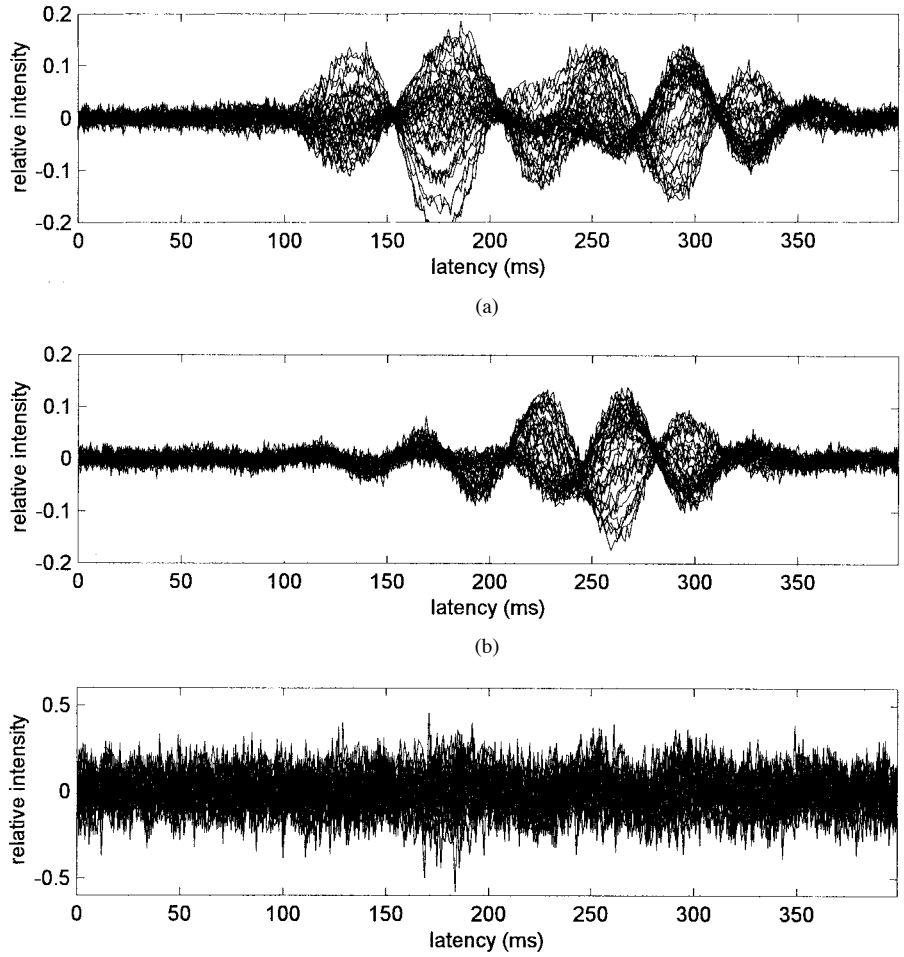

Fig. 3. The 37-channel overlapped display of the field waveform generated in the computer simulation in Section III-B: (a) the task condition, (b) the control condition, and (c) one of the 100 single-epoch data generated in the task condition. This data is used to obtain the results shown in Fig. 7(b).

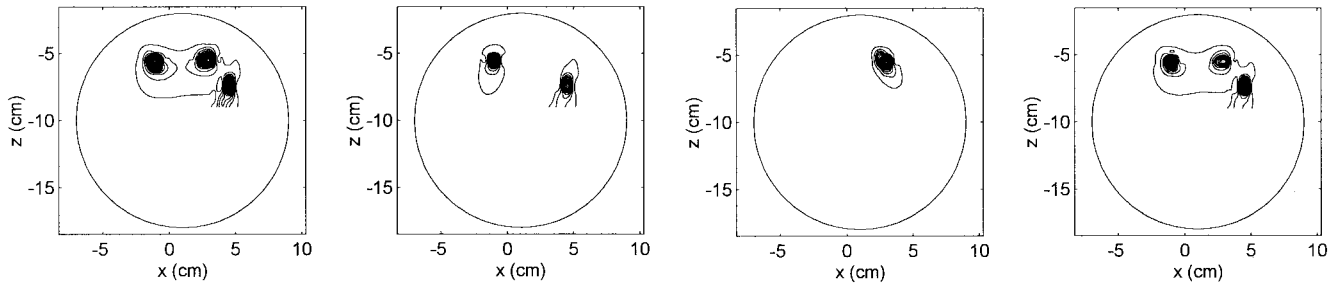

Fig. 4. Results of the MUSIC source localization when the task condition activates all three sources and the control condition activates the first and third sources: (a) Results of applying the standard MUSIC localizer [(7)] to the data obtained under the task condition, (b) results of applying (7) to the data obtained under the control condition, (c) results of the covariance difference analysis using (15), and (d) results of the simple waveform-subtraction method. The contours show the relative values of the localizer on the $y = 1.0$ plane, and each area where the localizer reaches a peak is considered to be the location of one dipole source. The circle is the boundary of the sphere used for the forward calculation, depicting the approximate size of a human brain on this plane.

second and third sources. In this case, the first source is the target source and the second source is activated only in the control condition. The source waveforms shown by the solid lines in Fig. 2(a), (b), and (c) were assigned to the first, second, and third sources both for the task and control conditions. The results obtained by applying the standard MUSIC localizer to the task and control data are shown in Fig. 6(a) and (b), respectively. According to the discussion in Section II-C, the covariance difference analysis should detect the control (the second) source as well as the target (the first) source. The results of the covariance difference analysis are shown in Fig. 6(c). In these results, the first and second sources are detected. We then estimated the matrix ΔQ by using (22); the diagonal elements were found to be 33.8 (the first source)

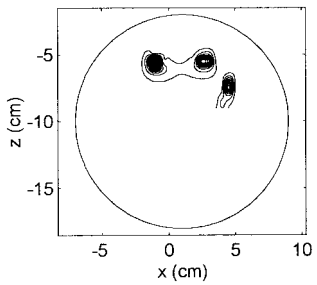

Fig. 5. The results of the covariance difference analysis when strong correlation exists between the task and control sources. The waveform shown in Fig. 2(a) was assigned to both the first and second sources in this computer simulation.

and -42.7[1] (the second source). The signs of these diagonal elements indicate that the first source is the target source and the second source is the control source. These results demonstrate the validity of the discussion in Section II-C.

E. Influence of Time Jitter in Control Source Response

It is possible that the onset of the control source response will have a time jitter and vary from epoch to epoch in actual cognitive experiments. In such cases, the proposed covariance difference analysis cannot effectively eliminate the control source influence if it is applied to the data obtained by averaging multiple epochs. The same computer simulation as described in Section III-B was again performed except that the onset of the control source in the task measurement was randomly changed within a maximum of 30 ms when generating data for each epoch. The covariance difference analysis was applied to the data averaged over 100 sets of these single-epoch data.

The results are shown in Fig. 7(a). Obviously, the control source influence was not eliminated. The results obtained when the covariance difference analysis was applied to a pair of the single-epoch data are shown in Fig. 7(b). One of the single epoch data used here is shown in Fig. 3(c). The results contain a severe blur, due to the low signal-to-noise ratio of the single epoch data, even though the control source influence was removed. This blur, however, can be reduced by averaging the difference matrix obtained using each set of single-epoch data. The results of using this averaged-difference matrix are shown in Fig. 7(c). To obtain these results,100 single-epoch difference matrices were averaged, and the proposed localizer [(15)] was calculated using this averaged difference matrix. The quality of these results is almost equal to that of the results in Fig. 4(c). Therefore, when one suspects that the onset of the control-source response may vary, the procedure mentioned in this subsection should be applied to eliminate the control source influence.

IV. Application to Evoked-Field Measurements Simulating Task- and Control-Type Experiments

We applied the proposed method to source localization for measured evoked responses; these measurements simulated task- and control-type experiments. The evoked responses were recorded using the 37-channel Magnes magnetometer installed at the Biomagnetic Imaging Laboratory, University of California, San Francisco. All measurements were done in a magnetically shielded room.

In these experiments we applied an auditory stimulus, a somatosensory stimulus, or both to a male volunteer. The auditory stimulus was a 1000-Hz pure tone with a 200-ms duration; it was applied to the subject's right ear. The somatosensory stimulus was a 30-ms-duration tactile pulse (17 psi) delivered to the distal segment of the right index finger. In the combination stimulus, the auditory and somatosensory stimuli started at the same time. These auditory, somatosensory, and combination stimuli were repeatedly given one after the other without changing the head position relative to the sensor array. The data was acquired at a sampling frequency of 1 kHz for the prestimulus interval of 300 ms and the poststimulus interval of 800 ms and averaged for 256 epochs of each stimulus condition. An on-line bandpass filter with a bandwidth from 1–400 Hz was used and no post-processing digital filter was applied. The sensor array was placed on the left hemisphere and positioned to best record the M100 auditory response. The mean interstimulus interval was 2 s, randomly varied between 1.75 and 2.25 s.

The x, y, and z coordinates used to express the localization results are depicted in Fig. 8. The results of applying the standard MUSIC algorithm are shown in Figs. 9, 10, and 11. The data from 0–300 ms post stimulus onset were used for the analysis. In these figures, the localizer shown in (7) was calculated with an interval of 0.5 cm within a volume defined as $-4 \leq x \leq 6$, $-3 \leq y \leq 6$, and $3 \leq z \leq 11$. These figures show the projections of the localizer values onto the transverse, coronal, and sagittal planes; the relative positions of these planes are shown in Fig. 8. The circles depicting a human head represent the projections of the sphere used to calculate the forward solutions.

The results obtained using the data measured with only the auditory stimulus are shown in Fig. 9. The sharp single peak corresponds to a source in the auditory cortex. The results from the somatosensory stimulus alone are shown in Fig. 10. Two sources, probably corresponding to sources at the primary (SI) and secondary somatosensory (SII) cortices, can be seen, although they are not well resolved. The results from the combination of auditory and somatosensory stimuli are shown in Fig. 11. Two peaks can be seen in the left hemisphere. The sharp peak probably corresponds to the source at SI; the dull peak probably corresponds to the two sources at the auditory and secondary somatosensory cortices; these two sources cannot be resolved because they are very close together.

We calculated two covariance matrices for the covariance difference analysis: one by using the data from the combined stimulus and the other by the data from the somatosensory stimulus. That is, the combined stimulus was assumed to be the task stimulus, and the somatosensory stimulus was assumed to be the control stimulus. The data portion from 0–300 ms were also used for calculating both of the two covariance matrices. The results of the covariance difference analysis are shown in Fig. 12. A single sharp peak exists at almost the

[1] These elements are expressed using an arbitrary scale.

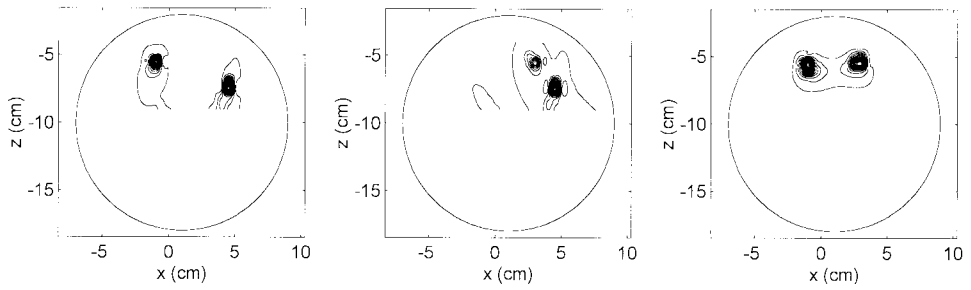

Fig. 6. Results of the MUSIC source localization when the task condition activates the first and third sources and the control condition activates the second and third sources: (a) Results for the data obtained from task condition, (b) results for the data from control condition, and (c) results of the covariance difference analysis using (15).

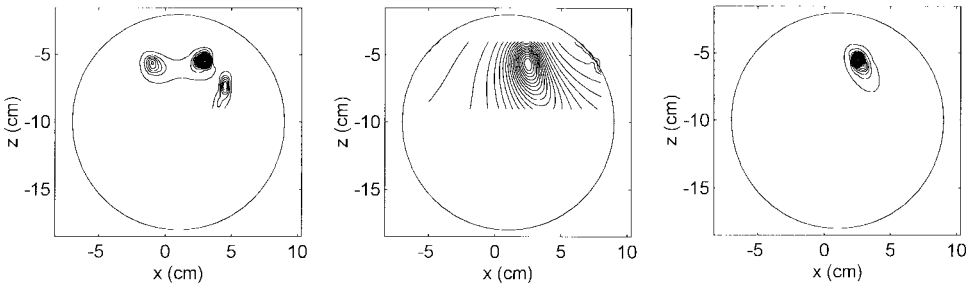

Fig. 7. Results of the same computer simulation as in Fig. 4 for the case when the onset of the control source response was randomly varied within 30 ms when generating each set of epoch data: (a) Results of the covariance difference analysis applied to the data obtained by averaging 100 sets of single-epoch data, (b) results of the covariance difference analysis applied to a pair of single epoch data, and (c) results when 100 single-epoch difference matrices were averaged, and the localizer in (15) was calculated using the averaged matrix.

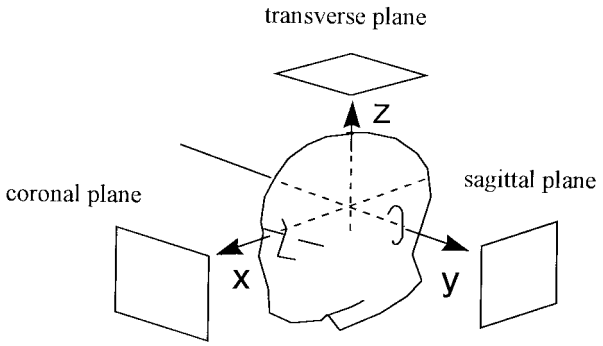

Fig. 8. The x, y, and z coordinates used to express the localization results shown in Figs. 9–12. The midpoint between the left and right preauricular points is defined as the coordinate origin. The axis directed away from the origin toward the left preauricular point is defined as the $+y$ axis, and that from the origin to the nasion is the $+x$ axis. The $+z$ axis is defined as the axis that is perpendicular to both these axes and directed from the origin to the vertex. The relative positions of the transverse, sagittal and coronal planes are also shown.

same location where the source from the auditory stimulus was localized (Fig. 9). These results clearly show that the covariance difference analysis can extract the target (auditory) source location and eliminate the disturbance from the control (somatosensory) sources.

V. Conclusion

As mentioned in Section III-B, a naive method to extract the information about the target activities is to simply subtract the magnetic-field waveform obtained by the control measurement from that by the task measurement. The advantages of the proposed covariance difference algorithm over this simple subtraction method are summarized as follows.

First, the simple subtraction method is effective only when the onset of the control-source time response in the task measurements is exactly equal to that in the control measurements. Otherwise, this method fails to extract the target-source information, as was shown in Fig. 4(d). Second, the simple subtraction method also cannot handle the case where some of the control sources do not appear in the task measurements. In this case, even if all sources are correctly localized, the simple subtraction method provides no procedure for discriminating between the target sources and the control sources. In contrast, covariance difference analysis can discriminate between these two types of sources by checking the signs of the diagonal elements of matrix $\widehat{\Delta Q}$ obtained using (22), as discussed in Section II-C.

The assumption that makes the proposed covariance difference analysis valid is that the brain response is linear, i.e. the brain responses to different stimuli are additive and the correlation between these responses is zero. It should be noted that the validity and the limitations of the linear modeling of brain response have been studied in the functional MRI [13], [14], and the linear modeling proves to be effective for analyzing the fMRI or PET data in ordinary measurement conditions [15], although the brain response is known to be, in principle, highly nonlinear.

The success of the proposed covariance difference analysis depends on the assumption that this linear modeling is also valid for MEG measurements. In actual MEG measurements,

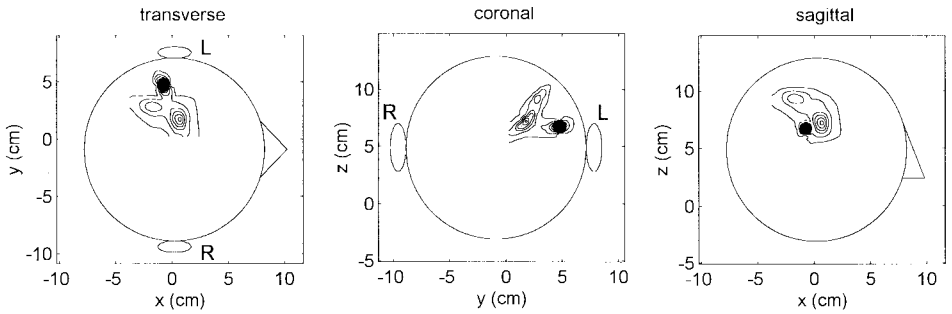

Fig. 9. Results of applying the standard MUSIC localizer in (7) to data obtained with the auditory stimulus. The localizer was calculated with an interval of 0.5 cm within a volume defined as $-4 \leq x \leq 6, -3 \leq y \leq 6$, and $2 \leq z \leq 10$; the projections of the localizer values onto the transverse, coronal, and sagittal planes are shown. The circles depicting a human head represent the projections of the sphere used to calculate the forward solution.

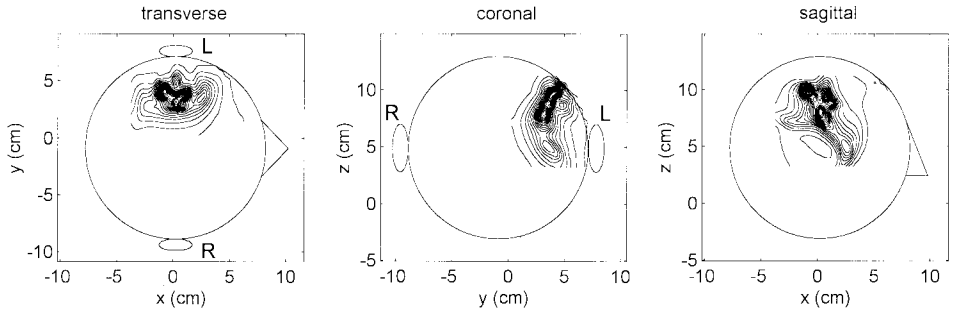

Fig. 10. Results of applying the standard MUSIC localizer in (7) to data obtained with the somatosensory stimulus.

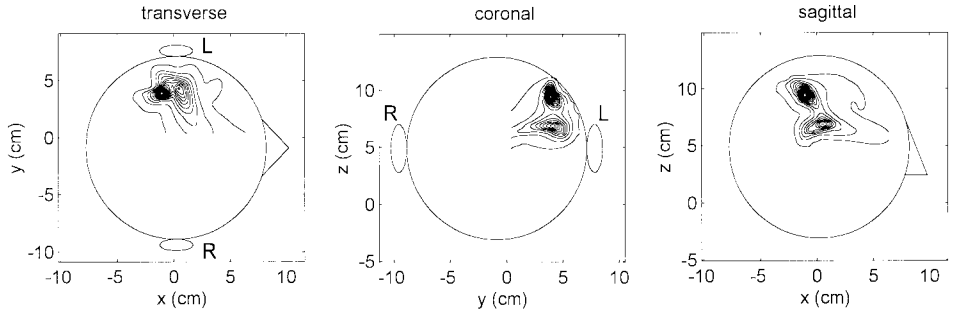

Fig. 11. Results of applying the standard MUSIC localizer in (7) to data measured with combination of the auditory and somatosensory stimuli.

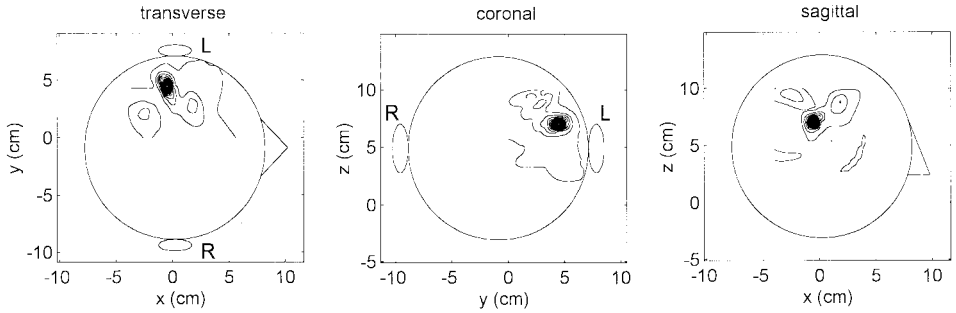

Fig. 12. Results of the covariance difference analysis. One covariance matrix was calculated from the auditory-somatosensory combined response and the other was calculated from the somatosensory response. The localizer in (15) was used.

however, this assumption may not always be valid, so the proposed method would not be effective in some cases. The validity and limitations of the linear model for the neuromagnetic measurements should be investigated, and the usefulness and limitations of the proposed method must be evaluated in such investigations.

In summary, we have proposed a method for extracting target source activities, which are of primary interest in experiments, by using two sets of evoked MEG data: one set measured by using task stimulus and the other by using control stimulus. The proposed method is a variant of the MEG-MUSIC algorithm, that is, a procedure similar to the MUSIC algorithm is applied to the difference between the two covariance matrices obtained from the above two measurements. Computer simulation showed the validity of the proposed method. Application to evoked-field measurements strongly suggested the method's effectiveness.

ACKNOWLEDGMENT

The authors wish to thank S. Masterman for helping to prepare the biomagnetic data. This work was carried out as part of the MIT–JST International Research Project "Mind Articulation."

REFERENCES

[1] M. Hämäläinen, R. Hari, R. J. IImoniemi, J. Knuutila, and O. V. Lounasmaa, "Magnetoencephalography-theory, instrumentation, and applications to noninvasive studies of the working human brain," *Rev. Mod. Phys.*, vol. 65, pp. 413–497, 1993.

[2] G. Romani, S. Williamson, and L. Kaufman, "Tonotopic organization of the human auditory cortex," *Sci.*, vol. 216, pp. 1330–1340, 1982.

[3] R. Hari, M. Hämäläinen, and S. L. Joutsiniemi, "Neuromagnetic steady-state responses to auditory stimuli," *J. Acoust. Soc. Amer.*, vol. 86, pp. 1033–1039, 1989.

[4] N. Fross, R. Hari, R. Salmelin, A. Ahonen, M. Hämäläinen, M. Kajola, J. Knuutila, and J. Simola, "Activation of the human posterior parietal cortex by median nerve stimulation," *Exp. Brain Res.*, vol. 99, pp. 309–315, 1994.

[5] R. Hari and R. Salmelin, "Human cortical oscillations: A neuromagnetic view through the skull," *Trends Neurosci.*, vol. 20, pp. 44–49, 1997.

[6] K. Sasaki, T. Tsujimoto, A. Nambu, R. Matsuzaki, and S. Kyuhou, "Dynamic activities of the frontal association cortex in calculating and thinking," *Electroenceph. Clin. Neurophysiol.*, vol. 74, pp. 58–75, 1989.

[7] M. J. Liu, P. B. C. Fenwick, J. Lumsden, C. Lever, K.-M. Stephan, and A. A. Ioannides, "Averaged and single-trial analysis of cortical activation sequence in movement preparation, initiation, and inhibition," *Human Brain Mapping*, vol. 4, pp. 254–264, 1996.

[8] A. Paulraj and T. Kailath, "Eigenstructure methods for direction of arrival estimation in the presence of unknown noise fields," *IEEE Trans. Acoust., Speech, Signal Processing*, vol. ASSP-34, pp. 13–20, 1986.

[9] J. C. Mosher, P. S. Lewis, and R. M. Leahy, "Multiple dipole modeling and localization from spatio-temporal MEG data," *IEEE Trans. Biomed. Eng.*, vol. 39, pp. 541–557, 1992.

[10] J. Sarvas, "Basic mathematical and electromagnetic concepts of the biomagnetic inverse problem," *Phys. Med. Biol.*, vol. 32, pp. 11–22, 1987.

[11] R. O. Schmidt, "A signal subspace approach to multiple emitter location and spectral estimation," Ph.D. dissertation, Stanford Univ., Stanford, CA, 1981.

[12] A. Paulraj, B. Ottersten, R. Roy, A. Swindlehusrt, G. Xu, and T. Kailath, "Subspace methods for directions-of-arrival estimation," in *Handbook of Statistics*, N. K. Bose and C. R. Rao, Eds. Amsterdam, the Netherlands: Elsevier Science, 1993, pp. 693–739.

[13] G. M. Boynton, S. A. Engel, G. H. Glover, and D. J. Heeger, "Linear analysis of functional magnetic resonance imaging in human V1," *J. Neurosci.*, vol. 16, pp. 4207–4221, 1996.

[14] K. J. Friston, C. J. Price, P. Fletcher, C. Moore, R. S. J. Frackowiak, and R. J. Dolan, "The trouble with cognitive subtraction," *Neuroimag.*, vol. 4, pp. 97–104, 1996.

[15] K. J. Friston, A. P. Holmes, K. J. Worsley, J.-P. Polin, C. D. Frith, and R. S. J. Frackowiak, "Statistical parametric maps in functional imaging: A general linear approach," *Human Brain Mapping*, vol. 2, pp. 189–210, 1995.

Kensuke Sekihara (M'88) received the M.S. degree in 1976 and the Ph.D. degree in 1987 both from Tokyo Institute of Technology, Tokyo, Japan

Since 1976, he has worked with Central Research Laboratory, Hitachi, Ltd., Tokyo, Japan. He was a Visiting Research Scientist at Stanford University, Stanford, CA from 1985–1986, and at Basic Development, Siemens Medical Engineering, Erlangen, Germany, in 1991–1992. He is currently working with "Mind Articulation" research project sponsored by Massachusetts Institute of Technology (MIT), Cambridge, and Japan Science and Technology Corporation, Tokyo, Japan. His research interests include the biomagnetic inverse problems, and statistical estimation theory, especially its application to noninvasive measurements of brain functions.

Dr. Sekihara is a Member of IEEE Medicine and Biology Society, IEEE Signal Processing Society, and International Society of Magnetic Resonance in Medicine.

David Poeppel obtained the B.S. and Ph.D. degrees in cognitive neuroscience at Massachusetts Institute of Technology (MIT), Cambridge, in 1990 and 1995, respectively.

He is currently an Adjunct Assistant Professor in the Department of Radiology, University of California San Francisco, and an Assistant Professor in the Departments of Linguistics and Zoology at the University of Maryland at College Park. His research uses the functional neuroimaging methods magnetoencephalography (MEG) and functional magnetic resonance imaging (fMRI) to investigate the neural basis of speech and language processing.

Alec Marantz received the B.A. degree in psycholinguistics from Oberlin College, Oberlin, OH, in 1978 and the Ph.D. degree in linguistics from the Massachusetts Institute of Technology (MIT), Cambridge, in 1981.

He joined the faculty at MIT in 1990, where he is currently Professor of Linguistics in the Department of Linguistics and Philosophy. His research interests include the syntax and morphology of natural languages, linguistic universals, and the neurobiology of language. He is currently involved in revising morphological theory within linguistics and in exploring MEG techniques to uncover how the brain process language.

Colin Phillips received the B.A. degree in modern languages from Oxford University, Oxford, U.K., in 1990 and the Ph.D. degree in linguistics from Massachusetts Institute of Technology (MIT), Cambridge, in 1996.

He is currently an Assistant Professor in the Department of Linguistics and the Program in Cognitive Science at the University of Delaware. His research combines theoretical linguistics with language processing, language acquisition and neurolinguistics, with the goal of embedding explicit linguistic theories in cognitively and neuroscientifically grounded models of language processes.

Hideaki Koizumi was born in Tokyo, Japan, in 1946. He was graduated from the Department of Pure and Applied Sciences, the University of Tokyo, Tokyo, Japan, in 1971. He joined Hitachi, Ltd. Tokyo, Japan, and received the doctoral degree in physics from the University of Tokyo in 1976 for his thesis: "Creating Polarized Zeeman-Effect Atomic Absorption Spectrometry."

He stayed as Visiting Faculty at the Lawrence Berkeley Laboratory, University of California, Livermore, CA, from 1978–1979. Upon returning to Japan, he led MRI development projects. He is a Chief Research Scientist at the Central Research Laboratory, Hitachi, Ltd. and a Professor of the Research Institute for Electronic Science, Hokkaido University, Sapporo, Japan. He now leads projects on environmental measurement and analysis, and noninvasive higher-order brain function analysis.

Dr. Koizumi is a Member of the Board of Directors of the Chemical Society of Japan. He received many awards such as the Ohkochi Memorial Prize, the Prize of Science and Technology Minister, and IR-100.

Yasushi Miyashita received the Ph.D. degree in physiology from the University of Tokyo, Japan, in 1979.

He is currently Professor and Chairman of the Physiology Department, the University of Tokyo School of Medicine, Tokyo, Japan. His research interests include neural basis of cognition in primates, functional imaging, and image processing with MRI, MEG, and optical devices.